REPORT DOCUMENTATION PAGE

Form Approved
OMB No. 0704-0188

PLEASE DO NOT RETURN YOUR FORM TO THE ABOVE ORGANIZATION.

1. REPORT DATE *(DD-MM-YYYY)*	2. REPORT TYPE	3. DATES COVERED *(From - To)*
11-05-2015	Conference Proceedings	

4. TITLE AND SUBTITLE

Near-infrared compressive line sensing imaging system using individually addressable laser diode array

5a. CONTRACT NUMBER

5b. GRANT NUMBER

5c. PROGRAM ELEMENT NUMBER

0602435N

6. AUTHOR(S)

Bing Ouyang, Weilin Hou, Frank M. Caimi, Fraser R. Dalgleish, Anni K. Vuorenkoski, Sue Gong, Water Britton

5d. PROJECT NUMBER

5e. TASK NUMBER

5f. WORK UNIT NUMBER

73-6892-A5-5

7. PERFORMING ORGANIZATION NAME(S) AND ADDRESS(ES)

Naval Research Laboratory
Oceanography Division
Stennis Space Center, MS 39529-5004

8. PERFORMING ORGANIZATION REPORT NUMBER

NRL/PP/7330--15-2573

9. SPONSORING/MONITORING AGENCY NAME(S) AND ADDRESS(ES)

Office of Naval Research
One Liberty Center
875 North Randolph Street, Suite 1425
Arlington, VA 22203-1995

10. SPONSOR/MONITOR'S ACRONYM(S)

ONR

11. SPONSOR/MONITOR'S REPORT NUMBER(S)

12. DISTRIBUTION/AVAILABILITY STATEMENT

Approved for public release, distribution is unlimited.

13. SUPPLEMENTARY NOTES

14. ABSTRACT

The compressive line sensing (CLS) active imaging system was proposed and validated through a series of test-tank experiments. As an energy-efficient alternative to the traditional line-scan serial image, the CLS system will be highly beneficial for long-duration surveillance missions using unmanned, power-constrained platforms such as unmanned aerial or underwater vehicles. In this paper, the application of an active spatial light modulator (SLM), the individually addressable laser diode array, in a CLS imaging system is investigated. In the CLS context, active SLM technology can be advantageous over passive SLMs such as the digital micro-mirror device. Initial experimental results are discussed.

15. SUBJECT TERMS

Compressive Sensing, DMD, Laser, Infrared Imaging, Individually Addressable Laser Diode Array

16. SECURITY CLASSIFICATION OF:			17. LIMITATION OF ABSTRACT	18. NUMBER OF PAGES	19a. NAME OF RESPONSIBLE PERSON
a. REPORT	b. ABSTRACT	c. THIS PAGE			Weilin Hou
Unclassified	Unclassified	Unclassified	UU	12	19b. TELEPHONE NUMBER *(Include area code)* (228) 688-5257

Reset

PUBLICATION OR PRESENTATION RELEASE REQUEST 15-1231-1574 Pubkey 9657 NRLINST 5510.40

1. REFERENCES AND ENCLOSURES

Ref: (a) NRL Instruction 5600.2
(b) NRL Instruction 5510.40E

Encl: (1) Two copies of subject publication/presentation

2. TYPE OF PUBLICATION OR PRESENTATION

( ) Abstract only, published	( ) Abstract only, not published
( ) Book author	( ) Book chapter
( ) Book editor	( ) Multimedia report
(X) Conference Proceedings (refereed)	( ) Conference Proceedings (not refereed)
( ) Journal article (refereed)	( ) Journal article (not refereed)
( ) Oral Presentation, published	( ) Oral Presentation, not published
( ) Video ( ) Poster	( ) Other, explain

ALL DOCUMENTS/PRESENTATIONS MUST BE ATTACHE

3. ADMINISTRATIVE INFORMATION

STRN NRL/PP/7330-15-2573
Route Sheet No 7330/
Job Order No 73-6892-A5-5
Classification U S C
FOUO
Sponsor ONR BASE 6.2, BK
Sponsor's approval yes* (attached)
(*Required if research is otheran 6.1/6.2 NRL or ONR unclassified research or if publication/presentation is classified

4. AUTHOR

Title of Paper or Presentation
Near-infrared compressive line sensing imaging system using individually addressable laser diode array

AUTHOR(s) LEGAL NAMES(s) OF RECORD (First, MI, Last), CODE, (Affiliation if not NRL).
Bing Ouyang Florida Atlantic Univ., Weilin Hou 7333, Frank Caimi Florida State Univ., F.R. Dalgleish Florida Atlantic Univ., A.K. Vuorenkoski Florida Atlantic Univ., Sue Gong Texas Christian Univ., Walter Britton Florida Atlantic University,

This paper will be presented at the SPIE DSS
(Name of Conference)
20-APR - 24-APR-15, Baltimore, MD, Unclassified
(Date, Place and Classification of Conference)
and/or for published in SPIE DSS, Unclassified
(Name and Classification of Publication) (Name of Publisher)

5. CERTIFICATION OR CLASSIFICATION

It is my opinion that the subject paper (is ____) (is not __x__) classified, in accordance with reference (b) and this paper does not violate any disclosure of trade secrets or suggestions of outside individuals or concerns which have been communicated to the NRL in confidence.

This subject paper (has ____) (has never __x__) been incorporated in an official NRL Report.

Weilin Hou, 7333 (Signature)
Name and Code (Principal Author) (Legal Name of Record and Signature Only)

6. ROUTING/APPROVAL (NOTE: If name other than your legal name of record is associated on the publication or presentation itself, add an explanatory note in the "comments" section below next to your signed legal name of record)

CODE	SIGNATURE	DATE	COMMENTS
Co-Author(s) Weilin Hou, 7333		5/1/15	Need by 14 May 2015
			This is a Final Security Review. Any changes made in the document, after approved by Code 1231, nullify the Security Review.
Section Head			
Branch Head Richard L. Crout, 7330		5-1-15	
Division Head Ruth H. Preller, 7300		5/1/15	1. To the best knowledge of this Division, the subject matter of this publication (has ____)(has never ____ Xbeen classified
			2. This paper (does ____) (does not __X__) contain any militarily critical technology.
ADOR/Director NCST E. R. Franchi, 7000			
DOR/CO			
Security, Code 1231		5/11/15	A copy of the paper, abstract or presentation is filed in this office
Associate Counsel,Code 1008.3	via Beede invention memo	5-19-2015	
Public Affairs (Unclassified/ Unlimited Only), Code 7030.4	Shannon Mensh	5-15-15	
Division, Code			
Author, Code			

HQ-NRL 5511/6 (Rev. 12/14) THIS FORM CANCELS AND SUPERSEDES ALL PREVIOUS VERSIONS

Near-infrared compressive line sensing imaging system using individually addressable laser diode array

Bing Ouyang*[1], Weilin Hou[2], Frank M. Caimi[1], Fraser R. Dalgleish[1], Anni K. Vuorenkoski[1], Sue Gong[3], Water Britton[1]

1. Harbor Branch Oceanographic Institute, Florida Atlantic University, 5600 US1 North, Fort Pierce, FL, USA 34946
2. Naval Research Lab,1005 Balch Blvd, Stennis Space Center, MS 39556
3. Department of Engineering, Texas Christian University, 2800 S University Dr., Fort Worth, TX 76129

*Tel. 772-242-2288, E-mail bouyang@hboi.fau.edu

ABSTRACT

The compressive line sensing (CLS) active imaging system was proposed and validated through a series of test-tank experiments. As an energy-efficient alternative to the traditional line-scan serial image, the CLS system will be highly beneficial for long-duration surveillance missions using unmanned, power-constrained platforms such as unmanned aerial or underwater vehicles. In this paper, the application of an active spatial light modulator (SLM), the individually addressable laser diode array, in a CLS imaging system is investigated. In the CLS context, active SLM technology can be advantageous over passive SLMs such as the digital micro-mirror device. Initial experimental results are discussed.

Keywords: Compressive Sensing, DMD, Laser, Infrared Imaging, Individually Addressable Laser Diode Array

1. BACKGROUND

The compressive line sensing (CLS) active imaging system [1, 2] was proposed as an energy-efficient alternative to the traditional laser line-scan (LLS) serial image [6, 9]. The non-adaptive serial raster-scan image formation in a LLS system can be a concern in certain situations. On unmanned aerial vehicles (UAVs) and unmanned underwater vehicles (UUVs) for which power is at a premium, the LLS sensor may consume significant power acquiring redundant data that will be discarded during the image compression phase. Another issue is that increased platform speeds will require lasers with higher repetition rates to maintain the same image resolution, which inevitably will increase the system cost and require more sophisticated noise mitigation.

By adopting the concept of resource compression, the CLS system aims to achieve faster signal formation, more flexible system configuration and higher energy efficiency. The technique also enables compact and robust system design. An experimental CLS prototype was constructed to conduct a series of test-tank experiments [3]. As in many other compressive sensing imaging applications, the experimental prototype was developed using a digital micro-mirror device (DMD). Although the experimental results validated the proposed CLS concept, they also revealed some limitations of adopting a passive spatial light modulation (SLM) device (i.e., the DMD) in such a system.

This paper investigates the power efficiency improvement using an emerging technology – Individually Addressable Laser Diode Array (IALDA) to in the CLS system.

.

We provide some theoretical foundations in Section 2 and introduce the IALDA devices in Section 3. In Section 4 we discuss the optical and electronic design of an IDALDA-based CLS system. In Section 5 we present some experimental results. Our conclusions are summarized in Section 6.

2. THEORETICAL FOUNDATIONS

2.1. Compressive Sensing and Distributed Compressive Sensing Theories

Compressive sensing (CS) is a framework for the simultaneous sampling and compression of sparse signals using incomplete linear measurements [5, 7]. A K-sparse signal $\boldsymbol{X} \in R^{N\times 1}$ (i.e., the projection of $\mathbf{X}$ on a sparsifying basis $\Psi \in R^{N\times N}$: $\boldsymbol{X} = \Psi\boldsymbol{\alpha}$ contains $K \ll N$ non-zero entries) can be recovered with overwhelming probability using more than $M = O(K \log N)$ incoherent linear measurements: $\boldsymbol{y} = \mathrm{A}\boldsymbol{X} = \mathrm{A}\Psi\boldsymbol{\alpha}$, when the measurement matrix $A \in R^{M\times N}$ is incoherent with the sparsifying basis Ψ and satisfies the Restricted Isometry Property (RIP) [5]. The vector α (and

Compressive Sensing IV, edited by Fauzia Ahmad, Proc. of SPIE Vol. 9484
94840I · © 2015 SPIE · CCC code: 0277-786X/15/$18
doi: 10.1117/12.2178804

therefore X) can be recovered from the measurements y by solving an $L1$-minimization problem. The CS theory essentially exploits the intra-signal redundancy within a single source, and there has been significant interest in extending it to cope with the inter-source correlations. One such approach is distributed compressive sensing (DCS). DCS is closely related to the distributed source coding theorems [13, 14], which hold that the minimum rate of encoding statistically dependent sources independently is the same as the minimum rate of encoding them jointly, when the sources are decoded jointly and their differences are Gaussian.

DCS attempts to exploit the inter-signal redundancy among distributed and correlated sources through the establishment of the proper joint sparsity models (JSMs) [4]. In JSM-1, the framework adopted in CLS, all sources $\boldsymbol{X}_l$ within the group consist of a sum of a common component $\boldsymbol{Z}_c$ and a component that is unique to each source Z_l: $\boldsymbol{X}_l = \boldsymbol{Z}_c + \boldsymbol{Z}_l$, $l = 0,1 \dots L$, where L is the number of signals to be solved jointly. On a sparsifying basis Ψ, $\boldsymbol{Z}_c$ and $\boldsymbol{Z}_l$ can be expressed as $\boldsymbol{Z}_c = \Psi\boldsymbol{\alpha}_c$, $\|\boldsymbol{\alpha}_c\|_0 = K_c$, and $\boldsymbol{Z}_l = \Psi\boldsymbol{\alpha}_l$, $\|\boldsymbol{\alpha}_l\|_0 = K_l$ and both are sparse, i.e., $K_c \ll N$ and $K_l \ll N$. The matrix form of the measurement model is illustrated below:

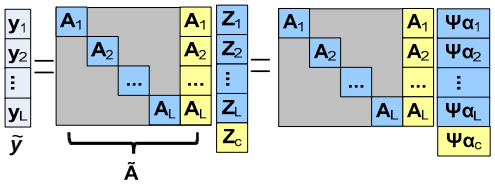

(1)

where $\tilde{\boldsymbol{y}} = [\boldsymbol{y}(1), \dots, \boldsymbol{y}(L)]^T \in R^{LM\times 1}$ are the measurements of L sources within the group; $\tilde{\boldsymbol{\alpha}} = [\boldsymbol{\alpha}(1), \dots, \boldsymbol{\alpha}(L)]^T \in R^{LN\times 1}$ are the coefficients of the sources on the sparsifying basis Ψ, and $\tilde{A}$ is the measurement matrix. Solving such a JSM-1 problem can be cast as $L1$ minimization with the cost function formulated by revising Equation (1) [4]:

$$\tilde{\boldsymbol{\alpha}}^* = \arg\min \|\boldsymbol{a}_c\|_1 + \|\boldsymbol{a}_1\|_1 + \cdots + \|\boldsymbol{a}_L\|_1 \quad \text{subject to } \|\tilde{\boldsymbol{y}} - \tilde{A}\Psi\tilde{\boldsymbol{a}}\|_2 \le \mathcal{E} \tag{2}$$

where $\|\boldsymbol{a}_l\|_1 = \sum_{i=1}^{N} |a_l(i)|$ is the $L1$-norm of $\boldsymbol{a}_l$.

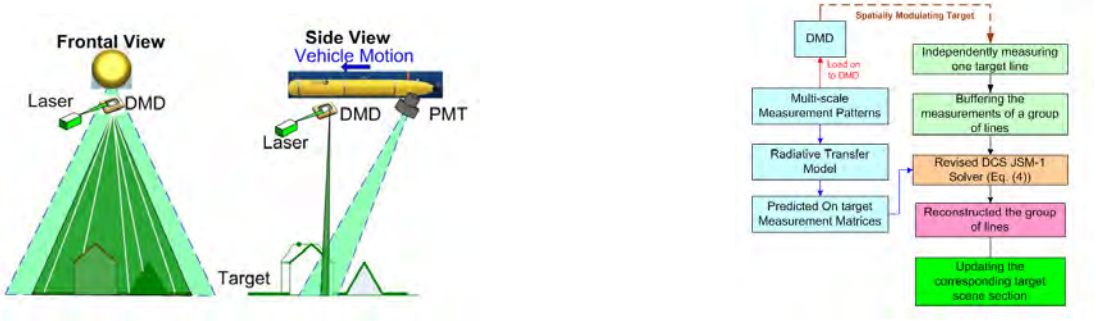

(a) CLS intensity imager (b) System processing flow

Figure 1. CLS imaging system architecture

2.2. CLS Imaging System Architecture

The CLS illuminator shares some similarity with the streak tube imaging Lidar [12], but instead of a one-dimensional (1D) fan beam, the illuminator projects a series of 1D fan patterns onto the current target line (Figure 2a). As in many CS imaging systems, this pattern can be generated through modulation of a laser source by an SLM device such as the DMD. Each pattern corresponds to one row in the CS measurement matrix (i.e., codebook). At the receiver, similar to the LLS system, a single element receiver such as the photomultiplier tube (PMT) records the total photon reflection corresponding to the modulation of the spatial pattern with the target as the measurement. Each line is measured independently; the platform motion enables the line-by-line sensing of the target scene. A group of lines are reconstructed jointly using the DCS JSM-1 model:

$$\tilde{\boldsymbol{\alpha}}^* = \arg\min \|\boldsymbol{a}_c\|_1 + \|\boldsymbol{a}_1\|_1 + \cdots + \|\boldsymbol{a}_L\|_1$$
$$\text{subject to } \|Y - \hat{\Phi}\Psi\boldsymbol{a}\|_2 \le \mathcal{E}, \quad X = \Psi\boldsymbol{a} \ge \mathbf{0} \tag{3}$$

where L is the group of lines to be solved jointly. One unique feature of this framework is that it shares some similarity with the "lucky imaging" scheme. Assuming the current line group parameter $L > 1$, then the reconstruction of line r will be included in L solutions. We will buffer these L solutions, and the optimum reconstruction for line r can then be derived from these L solutions (Figure 2b). One straightforward approach is to apply filtering such as a median filter to obtain the final solution: $\boldsymbol{a}_r^o = median[\boldsymbol{a}_r^u]$, for $u = 1 \ldots L$.

In the CLS system, resource compression is achieved by reducing the required measurements per line while still maintain desired image quality.

2.3. CLS Multi-scaled Illumination Patterns

Although a detailed discussion on the CLS signal model and reconstruction framework can be found elsewhere [1], it is useful here to discuss the illuminator patterns used in the CLS illuminator. These patterns are individual entries from the measurement matrix. To mitigate the forward scattering and backscattering, multi-scale binary dither patterns (Figure 2) are adopted. Each pattern is divided into N_b level-one blocks. Only one "on" pixel is present within each block, and its in-block location follows a uniform distribution. The on/off polarity of a block is determined by an independent Bernoulli random variable.

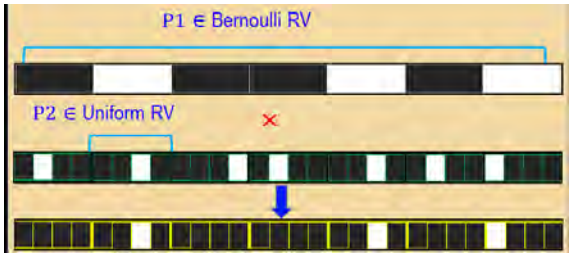

Figure 2. Multi-scale measurement matrix.

3. PASSIVE VS. ACTIVE SLM

3.1. DMD-based CLS Prototype System

Digital Micromirror Device (DMD) is a microelectromechanical (MEMS) device. A DMD consists of millions of electrostatically actuated micro-mirrors (or pixels) that can be individually controlled to reflect external light source. Figure 3 shows the light reflection paths when the pixels are at ON and OFF states [15]. When a pixel is at ON state, it tilts toward the light source and light is reflected to the projection lens. A bright pixel will show up in the projected image. While when a pixel is at OFF state, it tilts away from the light source and the light is directed to the light absorber. A dark pixel will be on the projected image. Since the entire DMD surface is under constant illumination, only part of the light is directed to the target when a binary pattern is generated using a DMD. The rest of the light is dissipated in the light absorber. Therefore, the energy efficiency of the illuminator using a DMD is lower when more dark pixels are in the projected binary patterns.

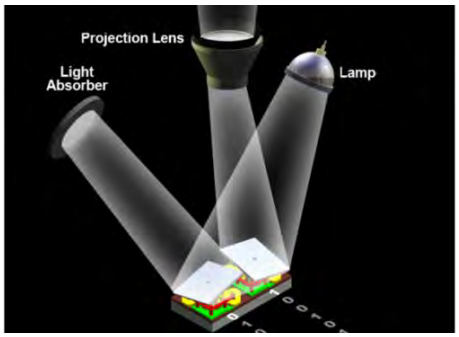

Figure 3. Pixels in ON and OFF states [15]

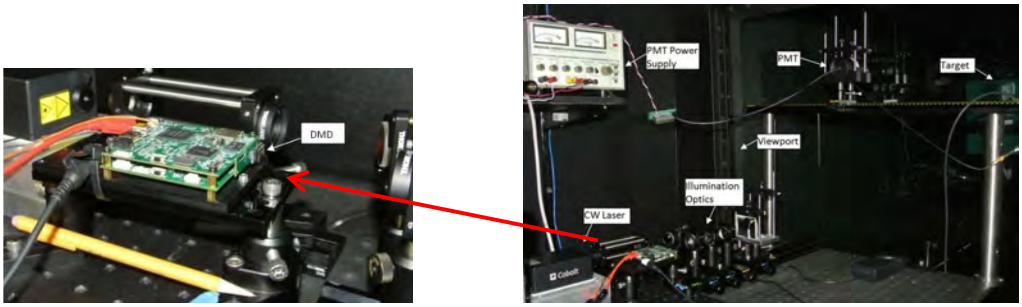

(a) DLP Lightcrafter (b) Overall prototype system

Figure 4. Initial prototype system [3]

A prototype system was developed to validate the aforementioned CLS concept [3] (Figure 4b). The prototype consists of the illumination and the receiver subsystems. The configuration of the receiver includes a single element detector such as a photomultiplier tube (PMT).

One of the main objectives of the optics in the illumination subsystem is to generate the required 1D spatial patterns. Two different options were explored (Figure 5a) – option 1: along the "on" reflection (i.e. projection) path (Figure 5b) and option 2: along the illumination path (Figure 5c). In both options the core component of the illumination subsystem is a compact DLP Lightcrafter evaluation module (Figure 4a). The prototype was used in the test-tank experiments and provided a valuable dataset to validate the CLS concept.

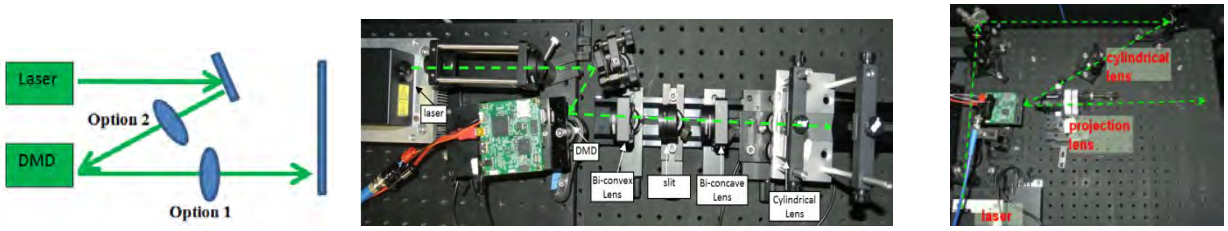

(a) Optical paths for the two options (b) Optical design for option 1 (c) Optical design for option 2

Figure 5. Options for illumination optics to generate 1D spatial patterns using DMD [3]

With the laser output set to 650 mw, in-water power was limited to 30mw for option 1 and 60 mw for option 2 with one-on/one-off binary patterns. Option 1 was mainly used in clear water experiments and option 2 was used in several turbidity cycle tests.

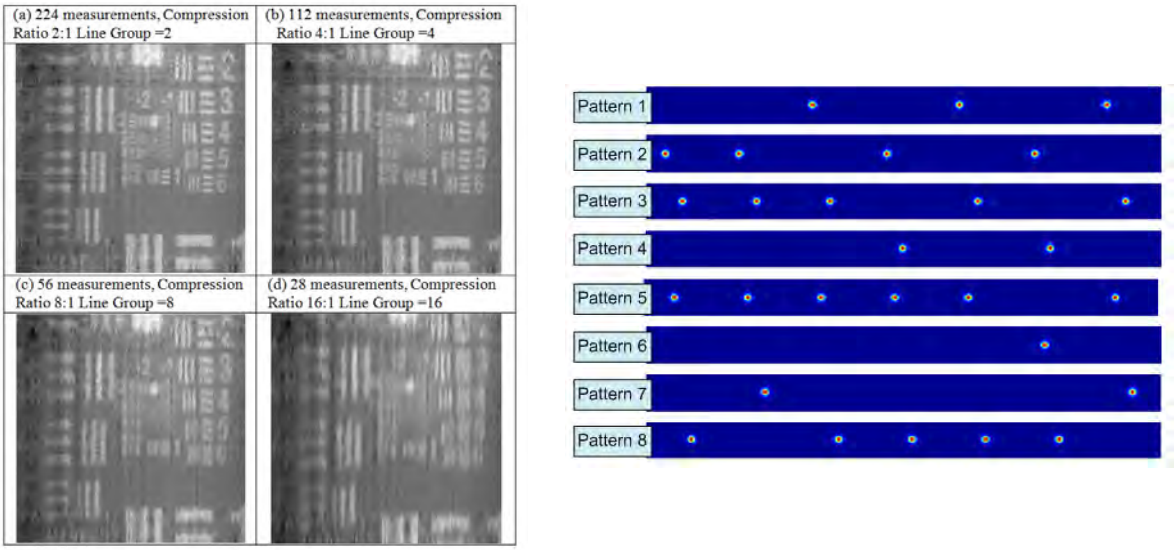

(a) Reconstructed images (b) Eight different sensing patterns used to acquire/reconstruct these images.

Figure 6. Image reconstruction using different compression ratios, line group setting with C=0.8 (4 Attenuation Lengths), and some corresponding sensing pattern examples with minimum spacing = 64 pixels

During this process, however, some issues with the DMD-based CLS prototype emerged. One issue is that the low laser power utilization. As discussed in section 2.3, increasing the distances between the minimum ON-pixels is one approach to mitigating forward scattering and backscattering. Figure 6a shows the reconstructed image from the dataset acquired in a higher turbidity test-tank experiment (C=0.8 with the target distance = 5m). The measurement patterns for this low-

visibility environment had a minimum ON-pixel spacing of 64 pixels (Figure 6b), and since only 1/64th of the mirrors were at ON-state, a significant amount light was lost.

Furthermore, although it is possible for DMD to control the amplitude (i.e., brightness) of different regions of the projected patterns through pulse-width modulation in a television or data projector system, it is not possible to achieve this when DMD is used as a passive binary SLM device.

We therefore want to discuss adopting an active SLM device – an IALDA – in the CLS imaging system.

3.2. Individually Addressable Laser Diode Array

The concept of using an IALDA as an SLM has been around since the 1990s [10]. In recent years, progresses in semiconductor laser diode manufacturing processes have enabled several different IALDA devices to reach the market. Most notables are the products from Quantel Laser [16] and Intense [17]. The Intense DLAM™ 200 was used in the experiments described here.

The DLAM 200 is manufactured using the so-called quantum well intermixing process [17], which allows for the monolithic integration of a large number of high-power, individually addressable, single-mode lasers on one chip (Figure 7). The on-board current driver application-specific integrated circuit is integrated with the IALDA to allow pixel control from a serial data input.

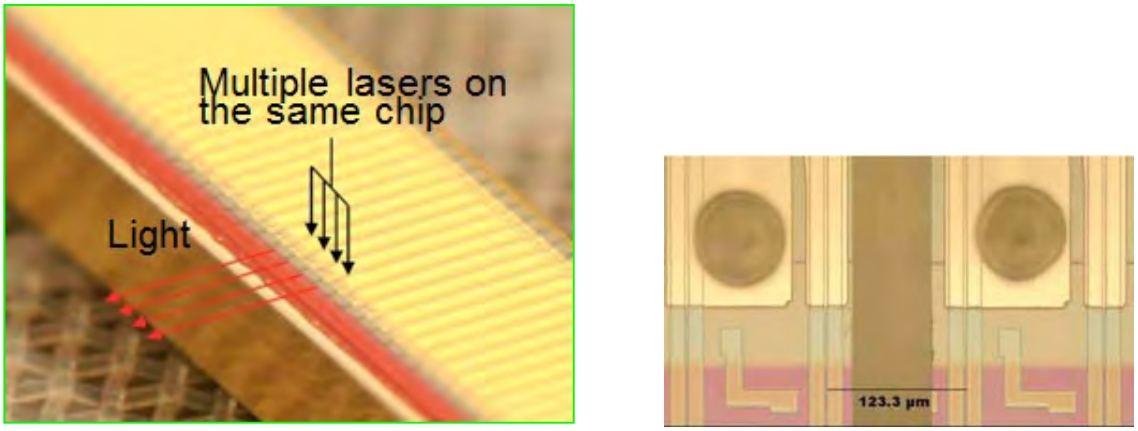

(a) DLAM 200 semiconductor device (b) Zoom-in view of two adjacent laser diodes

Figure 7. DLAM™ 200 individually addressable laser diode array [17]

Currently, IALDA devices are used in the printhead for non-contact laser marking and printing applications such as fruit labeling [8]. There are several features of these devices make them attractive to be used as the illuminator in a CLS system. First of all, each laser diode of the IALDA device can be turned on and off independently, which can mitigate the aforementioned low power utilization issue, and produce patterns with high contrast ratio. Secondly, DLAM 200 has a much higher pattern refresh rate (10MHz vs. 32KHz for the DMD). Lastly, the amplitude of each diode can be updated at a rate of 600Hz, which is sufficient to adjust the diode power level to compensate for the variation across the receiver field of view, as experienced in [3]. However, as an emerging technology, it has limitations to be used as the illuminator in the CLS system. For example, the shortest pulse width of the device is 100ns and the capable resolution (diode counts) is still low. The diodes on the current DLAM chip are limited to a one-dimensional array of 300 diodes. In addition, these devices are generally available only in near infrared (NIR) spectrum, mainly driven by the requirement from the laser printing market. Although it is ideal for many aerial active imaging applications, this spectrum is not suitable for underwater applications.

The pros and cons of the active SLM devices compared to the passive SLM devices (DMD) are summarized in Table 1.

Table 1. A Comparison of DMD and IALDA

	Pros	Cons
DMD	• High resolution (4K) • Capable of narrow pulses <1 ns • 2D array	• Throw away > 50% light • Unable to independently control the phase/amplitude of each pixel
IALDA	• Phase/amplitude/frequency of each pixel can be controlled independently • Fast update rate (up to 10 MHz)	• Long pulse ~100 ns • Low resolution (currently <300 emitters) • 1D array

4. DEVELOPMENT AND VALIDATION OF A IALDA-BASED CLS PROTOTYPE

We developed the CLS prototype subsystem using a DLAM™ 200-based LEONARDO printhead. LEONARDO is a turnkey 64 emitter computer-to-plate module offered by Intense (Figure 8). The laser wavelength is 808 nm and the peak power of each emitter is 168 mw. LEONARDO provides two data and control interfaces: a command interface (CI) via RS-422 serial connection and a high–speed-data-interface (HSDI) via a Displayport connection. The laser driver current (i.e., emitter amplitude) can only be controlled through the CI interface supporting a 115.2 KHz baud rate. Therefore, the amplitude of each emitter can be updated at a fairly high rate, if needed. The image data (i.e., binary pattern of the emitter array) can be updated through the HSDI interface at the fixed 1.25 Gbs rate. Therefore the patterns can be refreshed at a rate of up to 10 MHz.

Figure 8. LEONARDO computer-to-plate module

4.1. Electronic Design

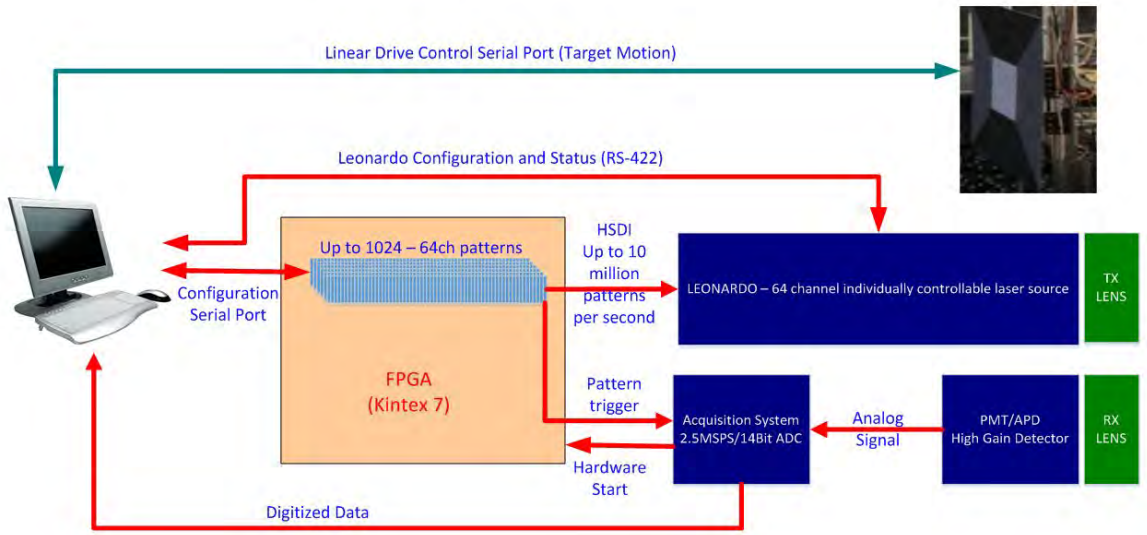

Figure 9. Electronic system block diagram

Figure 9 describes the electronic system block diagram. One major effort in the electronic system development was to program a Xilinx Kintex-7 FPGA KC705 Evaluation Kit. The KC705 communicates with the LEONARDO module through the HSDI interface for high-speed image data updating. For each pattern update, KC705 provides a trigger signal through an AES-FMC-DVI-G daughter board to one of the analog input ports on the National Instruments 6133 data

acquisition system. The control PC also communicates with the KC705 through the serial port to 1) configure the KC705 operation mode (i.e., pattern update frequency, single step vs. continuous pattern refreshing, etc.) and 2) pre-load image data (up to 1024 patterns). The analog output of the single-element detector (PMT or avalanche photodiode) connects to a separate analog input of the 6133 board.

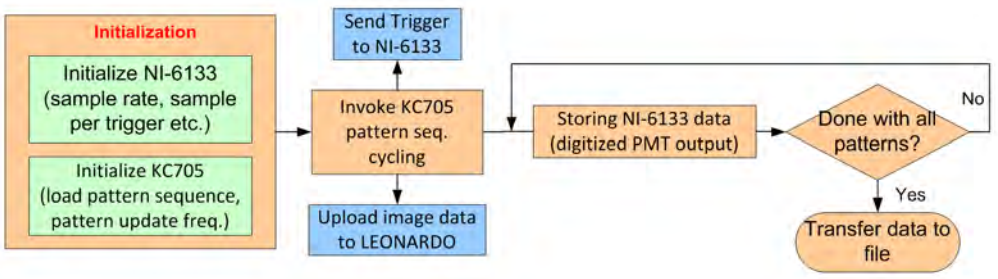

Figure 10. Data acquisition process flow

Figure 10 outlines the system operation flow. A Matlab script running on the PC is the central control. NI-6133 and KC705 are first initialized. KC705 is then instructed to start the pattern sequence cycling. During this step, new image data will be sent to the LEONARDO module and a trigger signal will be send to the NI-6133. The digitized data for each pattern will be buffered. Data will be transferred to file storage after the system cycles through all the pre-loaded patterns.

4.2. Optical Design

The other challenge in the system development is the optical design. LEONARDO is configured such that the internal bulk optics will focus the beam to a working distance of 150mm for printing applications. For the CLS prototype it is necessary to have collimated beams delivered at a much longer distance. The ideal choice would be a complete redesign of the optical frontend, but in the absence of the significant time and engineering resources this would require, we have elected to add external optics to collimate the beams.

As with most other laser diodes, the DLAM 200 emitter produces an elongated beam. The stretching along the slow axis is even more prominent when the beams are beyond the focal plane of the bulk optics (Figure 11).

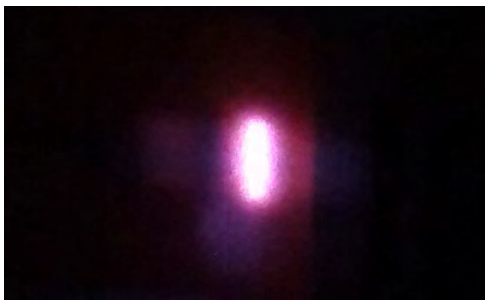

D= focal plane+100mm

D= focal plane+200mm

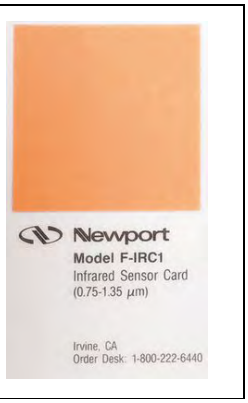

Figure 11. Beam at two different distances beyond the focal plane of the bulk optics (imaged using a Newport NIR Sensor Cards)

We made two different attempts to collimate the beam. In the first approach we used a single 2 in. plano-convex lens with 50mm focal length (fl), since our Zemax model seemed to indicate that such configuration is valid. However, the issue we discovered is that while the beams near the center of the lens were collimated well, on the edges the beam was significantly distorted into a “c” shape.

We therefore adopted the more traditional way of using a pair of cylindrical lenses to shape the slow axis and fast axis independently. To mitigate the issue of beam divergence along the fast axis, we used plano-concave cylindrical lenses

instead of plano-convex lenses. An fl=150 mm lens is used to collimate the beams along the fast axis and an fl=100 mm lens is used along the slow axis. We added a slit to further shape the beam along the slow axis. Figure 12 illustrates the optical system design.

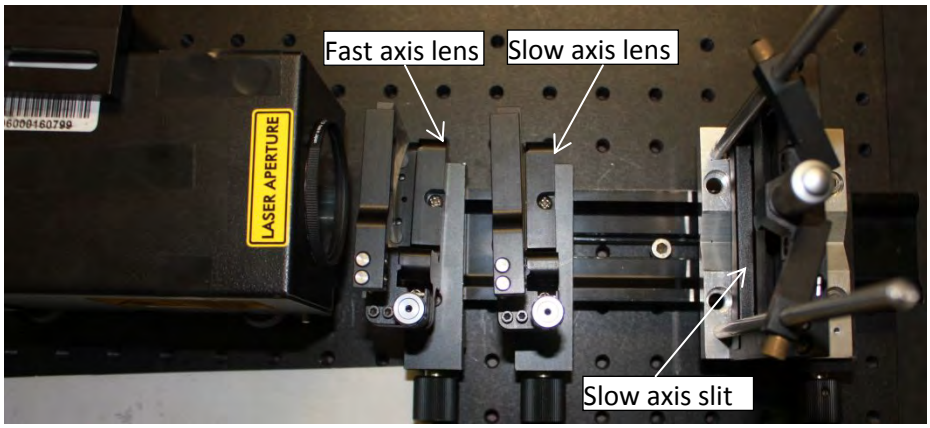

Figure 12. Beam collimation using a pair of plano-concave cylindrical lenses and a slit

Figure 13 shows some of the resulted patterns at 5m distance. The images were taken using a modified Canon Rebel Xti modified to acquire infrared scene. Each laser beam spot is estimated to be 8 mm at 5 m distance.

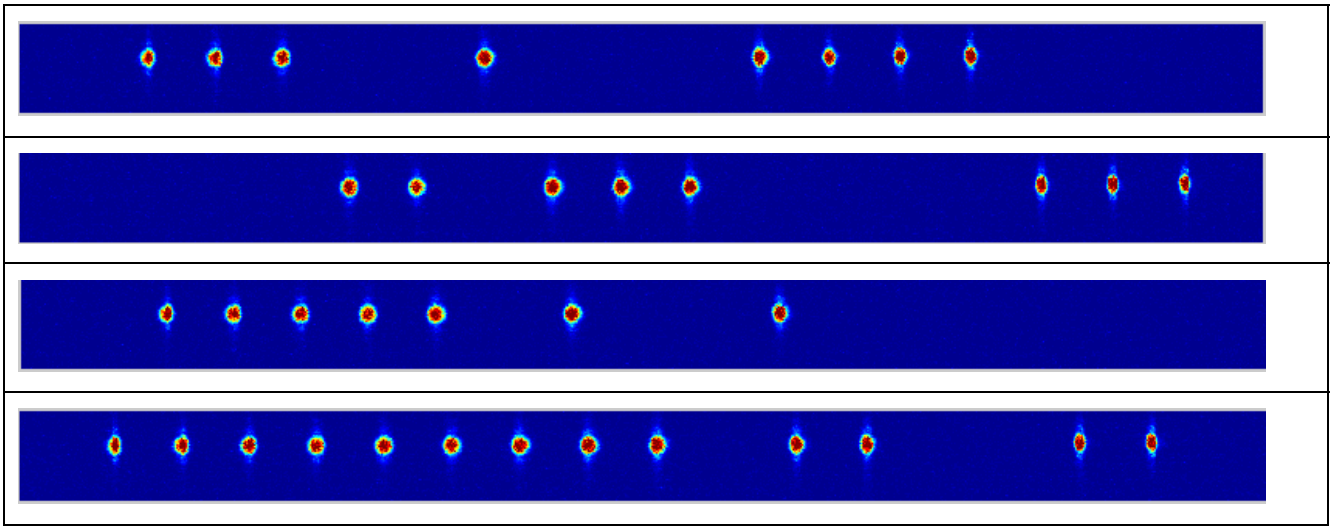

Figure 13. Four different illumination patterns projected using the beam collimation optics in Figure 12 (recorded using a Canon Rebel Xti camera modified to acquire infrared images)

4.3. System Calibration

A related issue is to calibrate the module so that the laser power from all emitters is more uniform. Although the vendor provided a default factory calibration, it was oriented toward achieving power uniformity at the focal plane of the bulk optics in the LEONARDO module. For the CLS prototype, the goal of the calibration is to achieve power uniformity at the receiver. The following calibration configuration (Figure 14) was therefore adopted: All emitters were set to the same pre-defined power setting, and the diodes were turned on one at a time to scan through a uniform target (blackboard). With one diode (i.e., center emitter 32) selected as the reference, the measured detector output offsets between the other emitters and the reference were used to adjust the settings.

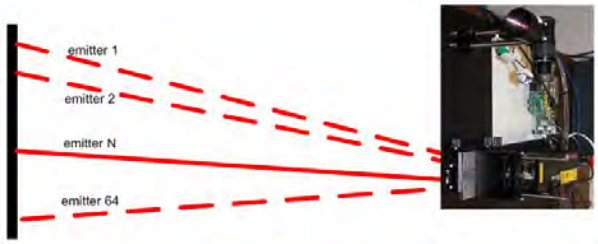

Figure 14. Illustration of the target calibration setup.

Figure 15 shows the detector power output before and after the calibration.

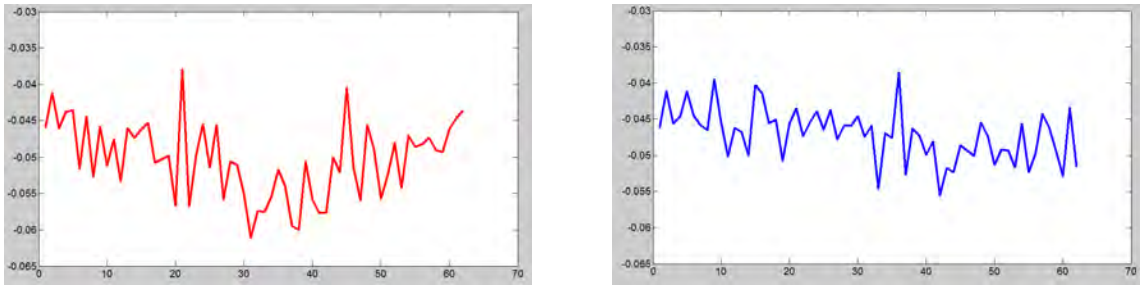

(a) Pre-calibration detector output (b) Post-calibration detector output

Figure 15. Pre/post calibration detector power output against a uniform target

While it is encouraging to notice the calibration process reduced the bias in the pre-calibration curve (Figure 15a), the improvement of the emitter-to-emitter variation was not as significant.

5. INITIAL VALIDATION TEST RESULTS

We conducted a series of experiments to obtain some initial validation of the prototype. In the first set of experiments, the setup was similar to that used in the calibration process (Figure 14). The target was placed 5 m from the illumination/receiver assembly shown in Figure 16a. We attempted to measure and reconstruct a single line segment. A Hamamatsu R928 PMT was used in the receiver due to its low cost and fairly high quantum efficiency in the NIR spectrum (Figure 16b). An 808nm bandwidth filter was place in front of the PMT to reduce the interference from the ambient light.

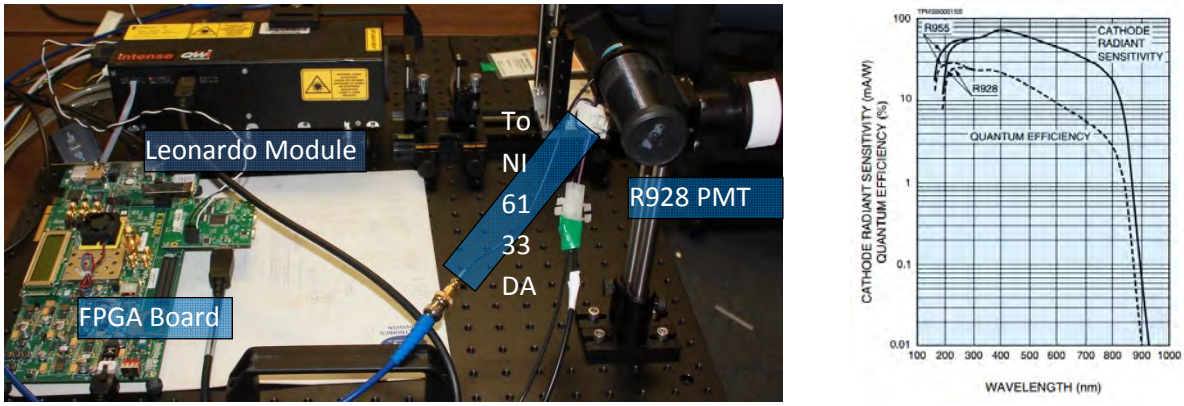

(a) Illuminator/Receiver Assembly (b) R928 PMT Response Curve

Figure 16. The Illuminator and Receiver Assembly Used in the Experiments and the PMT Response Curve

Figure 17 illustrates the results of two different targets: one containing two Gaussian curves and a second containing three stripes. The image reconstruction process is outlined elsewhere [1]. For this exercise, we used 32 measurements to reconstruct a 64x1 signal, a compression ratio of 2:1.

	Target image	Reconstruction Results
Two Gaussian Curves	 (a)	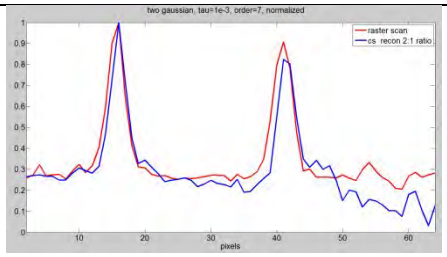 (b)
3 Stripes	 (c)	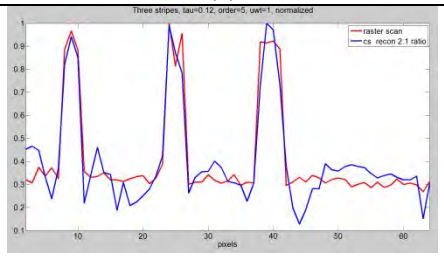 (d)

Figure 17. Initial validation test results using the IDLDA-based CLS prototype. The raster-scanned signal (64x1) is compared with the CS reconstruction using 32 measurements (2:1 compression)

For comparison we also raster-scanned the same line to be used as a reference (red curves in Figure 17b and Figure 17d) versus the signals reconstructed using the CLS framework (blue curves in Figure 17b and Figure 17d). The signals are normalized against their maximum values. It is therefore encouraging that the CS-reconstructed signals in general followed the raster scan signals well.

(a) IALDA-CLS Prototype

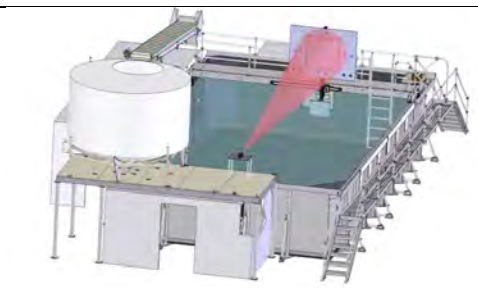

(b) CAD rendering of the above water platform in the HBOI optical test facility

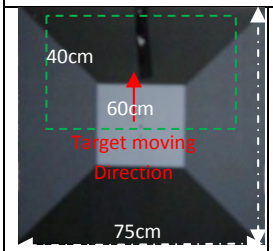

(c) Geometry Target

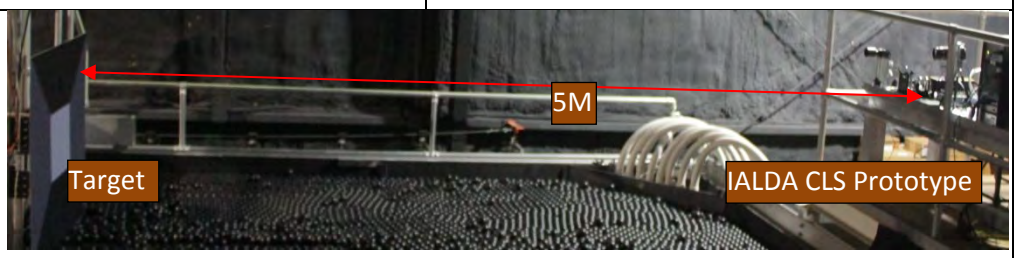

(d) Experiment setup

Figure 18. The setup using the above-water test platform at HBOI optical test facility to conduct the second validation test

For the second test we moved our prototype on the newly upgraded above-water test platform at the Harbor Branch optical test facility (Figure 18b). The illuminator and receiver assembly (Figure 18a) remained the same. The target was a 75 cm^2 geometric pattern attached to a linear drive capable of 5 degrees of freedom (Figure 18c). The area marked by the green dash lines is the actual region sensed by the imaging system during the experiment. The horizontal width of the region was estimated to be 60 cm. The linear drive was controlled to cover a vertical distance of 40 cm at a step size of 8 mm. The center 36 lines were included in the reconstructed image in Figure 19 below, resulting in an image size of 64x36. The top and bottom 7 lines were not included because the maximum line group was 7. This ensures that the image sizes at all compression ratios are the same. Figure 19 shows the reconstructed image at different compression ratios and sensing patterns, with either minimum ON-pixel spacing of 4 (i.e., at most 16 emitters will be turned on) or 8 (i.e., at most 8 emitters will be turned on).

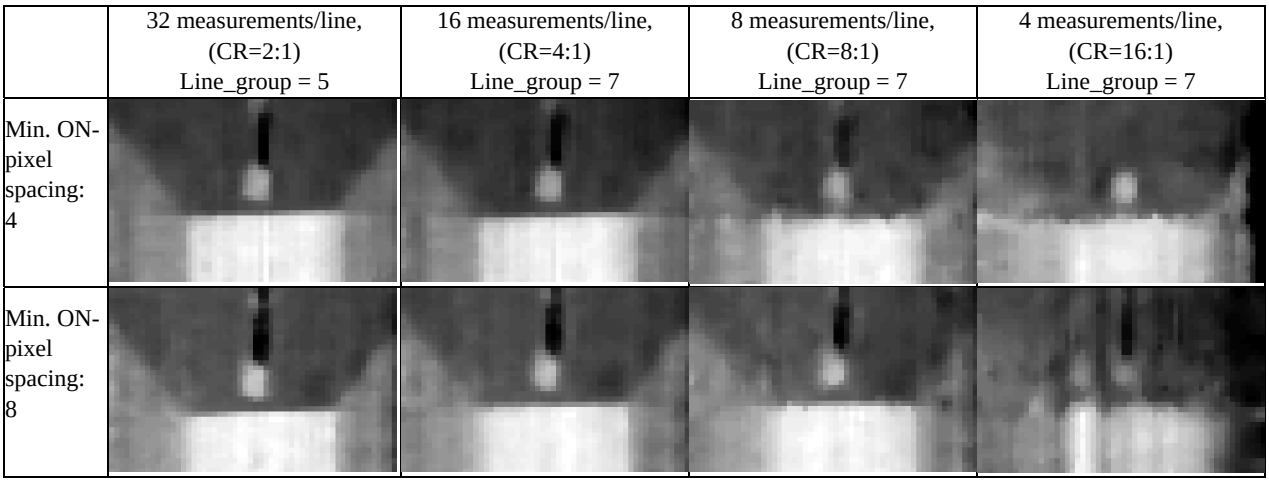

Figure 19. Reconstructed image at different compression ratios using two types of measurement patterns with different minimum spacing.

Both spacing options produced similar images at lower compression ratios (1:2 and 1:4), but as the ratios increased, dense spacing produced higher quality imagery. This was expected because these initial tests were conducted in air at a fairly close range.

It is also interesting to note that while the image intensity in general was consistent with the target under visible lighting conditions, a piece of black tape used to cover underlying mounting screws seemed to generate some new features under NIR lighting. This is evident by comparing the images taken with a regular camera (Figure 20a) and a modified camera capable of capturing the NIR illumination patterns (Figure 20 b and c). Both the upper and lower marked regions appear darker than their surround regions under visible lighting. However, the lower region actually reflects NIR lighting more strongly than the surrounding area.

(a) Under visible light (b) IR illuminating top segment of the tape (c) IR illuminating bottom part of the tape

Figure 20. Comparison of different feature under visible and NIR lighting

6. CONCLUSIONS

In this paper we proposed to adopt a type of active SLM device, the individually addressable laser diode, in our compressive line sensing imaging system. This is mainly aimed at improving the power efficiency, especially when more sparse patterns are needed such as in a strong scattering environment. The benefits and drawbacks of IALDA and passive SLM devices (e.g., digital micromirror device) were analyzed. We discussed the effort of developing such a prototype by

converting a LEONARDO module originally used in laser printing applications. Interestingly, the original application of the DMD also was printing. Although the initial tests validated the applicability of the IALDA in CLS, they also revealed some issues to be resolved. The beams in general were well collimated, but the laser beam spot was not uniform, which indicates the need for optical design improvement. The calibration process also needs to be improved. The low image resolution was expected due to the low emitter count, and although this could be improved by using IALDAs with high emitter counts, a more interesting approach that will be explored in future work is to integrate IALDA with a passive SLM device such as the DMD.

ACKNOWLEDGEMENT

This work was support by 2013 AFOSR Young Investigator Program, Naval Research Lab contract N00173-15-P-0263, HBOI internal funding and TCU Invest Scholar Fund. The authors want to thank Mr. Ben Metzger for the help during all phases of the experimental tests.

REFERENCES

[1] B. Ouyang, F. R. Dalgleish, F. M. Caimi, T. E. Giddings, W. Britton, A. K. Vuorenkoski, and G. Nootz, “Compressive Line Sensing Underwater Imaging System”, SPIE Optical Engineering Vol. 53, Issue 5, April 2014.

[2] B. Ouyang, F. R. Dalgleish, F. M. Caimi, T. E. Giddings, J. J. Shirron, A. K. Vuorenkoski., G. Nootz, W. Britton and B. Ramos, “Compressive Sensing Underwater Laser Serial Imaging System”, Journal of Electronic Imaging, special edition on Compressive Sensing, Vol. 22, Issue 2, 2013.

[3] B. Ouyang, F. M. Caimi, F. R. Dalgleish, A. K. Vuorenkoski and W. Hou, “Experimental studies of the compressive line sensing underwater serial imaging system”, SPIE Proceedings Vol. 9111, 2014.

[4] D. Baron, M. B. Wakin, M. F. Duarte, S. Sarvotham, and R. G. Baraniuk, “Distributed compressed sensing”, Rice University, Depart. Electrical and Computer Engineering Technical Report TREE-0612, Nov 2006.

[5] E. Candes, J. Romberg, and T. Tao, "Stable Signal Recovery from Incomplete and Inaccurate Measurements," Comm. Pure Appl. Math., vol. 59, pp. 1207-1223, 2006.

[6] F. R. Dalgleish and F. M. Caimi, “Synchronous Laser Line Scanners for Undersea Imaging Applications,” Taylor and Francis series in Optical Engineering (Laser and Optical Scanning), Chapter 16, 2010.

[7] D. Donoho, “Compressive Sensing,” IEEE Trans. Inform. Theory, vol. 52, pp. 1289-1306, 2006.

[8] S. Gorton and S. Howarth, "Laser diode arrays revolutionize fruit labelling", Industrial Lasers Solutions, May 2010.

[9] J. S. Jaffe, "Computer modeling and the design of optimal underwater imaging systems", IEEE J. Oceanic Eng., 15(2), 101-111, 1990.

[10] D. Kessler and J. G. Endriz, "Optical means for using diode laser arrays in laser multibeam printers and recorders", U.S. Patent 5,745,153, April 28, 1998.

[11] T. J. Kulp, D. Garvis, R. Kennedy, T. Salmon, K. G. Cooper, "Development and testing of a synchronous-scanning underwater imaging system capable of rapid two-dimensional frame imaging,", Appl. Opt. Jul 1;32(19):3520-30, 1993.

[12] B. C. Redman, A. J. Griffis, and E. B. Schibley, “Streak Tube Imaging Lidar (STIL) for 3-D Imaging of Terrestrial Targets,” Proc. of 2000 Meeting of the MSS Specialty Group on Active E-O Systems, 11–13, 2000.

[13] D. Slepian and J. K. Wolf, “Noiseless coding of correlated information sources”, IEEE Trans. Inform. Theory, vol. 19, pp. 471–480, July 1973.

[14] A. D. Wyner and J. Ziv, “The rate-distortion function for source coding with side information at the decoder”, IEEE Transactions on Information Theory, Jan, 1976.

[15] “DMD 101: Introduction to Digital Micromirror Device (DMD) Technology”, (n.d.) Retrieved May 1, 2011, from http://www.ti.com/lit/an/dlpa008a/dlpa008a.pdf.

[16] “Individual addressable laser diode array (IALDA)”, (n.d.), Retrieved April 15, 2014 from http://www.quantel-laser.com/products/item/individual-addressable-laser-diode-array-.html

[17] O. P. Kowalski, "The Development of Laser Diode Arrays for Printing Applications", April 25, 2012, Retrieved July 15, 2014, http://cdn.intechopen.com/pdfs-wm/35935.pdf.